Crimson Publishers
Wings to the Research

Research Article

Plant-Mediated Synthesis of Silver Nanoparticles and Antibacterial Activity on Implicated Biomolecules of Green *Spinicia Oleracea* Leaf Extract

Mohammed RA[1]*, Saleh GM[2] and Mutlak FA[1]

1College of Science Department of Physics, Iraq

2College of Science Department of Biology, Iraq

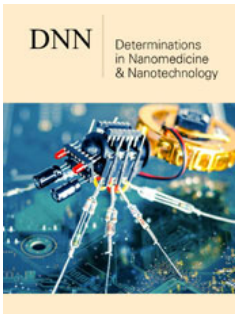

***Corresponding author:** Ruaa A Mohammed, College of Science Department of Physics, Baghdad, Iraq

Submission: February 2, 2022

Published: April 20, 2022

Volume 2 - Issue 4

How to cite this article: Mohammed RA*, Saleh GM and Mutlak FA. Plant-Mediated Synthesis of Silver Nanoparticles and Antibacterial Activity on Implicated Biomolecules of Green *Spinicia Oleracea* Leaf Extract. Determ in Nanomed & Nanotech. 2(4). DNN. 000544. 2022.

Copyright© Mohammed RA, This article is distributed under the terms of the Creative Commons Attribution 4.0 International License, which permits unrestricted use and redistribution provided that the original author and source are credited.

Abstract

This study used green spinach leaf extract for the green synthesis (monocolors) of silver nanoparticles (AgNPs). This search focuses on the optimization of synthesis by evaluating the impact on the each of the size distribution and activity of antibacterial against bacteria (*Escherichia coli*) of the green spinach leaf extract volume percent. The characterization of AgNP's was carried out utilizing UV-Visible spectrophotometers, size examination of particles, transmission electron microscopes, energy spectrometry with dispersion X rays, Fourier infrared spectrometer transform and x-ray scanning methods. The experimental data show that AgNPs have been produced effectively and size of particle is controlled by the amount of green spinach leaf extract. With the size reaching (5nm, polydispersity indices=0.063nm), the smaller volume percentage creates AgNPs with a spherically formed reach of 20%. The synthesized AgNPs by the spinach leaf extract had a good antibacterial activity especially at the concentration of (500µg/ml) in which the inhibition zone reached 35mm against gram negative bacteria *Escherichia coli*.

Keywords: *Spinicia oleracea* extract; AgNP's synthesis; Antibacterial activity

Abbreviations: ZnONP: Zinc Oxide Nanoparticles; PtNPs: Platinum Nanoparticles; TEM: Transmission-Electron Microscope; XRD: X-Ray Diffractors; SPR: Surface Plasm Resonance; DNA: Deoxyribonucleic Acid; NPs: Nanoparticles

Introduction

The use of plants' extract for the production of metal nanoparticles is an emerging technology that is extensively explored in the past several years with a view to replacing dangerous and non-renewable chemicals. Green production of nanoparticles in recent years has been an intriguing subject [1]. The fundamental concept of synthesis is the capacity to reducing metal ion precursors by flavonoids and alkaloids. Certain metal and metal oxide nanoparticles, for example silver nanoparticles [2], gold nanoparticles [3,4], Zinc Oxide Nanoparticles (ZnONP), [5] and Platinum Nanoparticles (PtNPs), are created via the redactor of plant extract [6]. AgNP green synthesis production is intriguing since several research have shown synthesized nanoparticles' features as a function of the plant extract type, content, and synthesis methods. The antibacterial, anti-fungal, anticancer and antioxidant effects of green synthesized AgNPs are claimed to have occurred. AgNPs' activity, physical, and chemical characteristics are influenced by their shape and form, which are influenced by the plant extract employed, composition, and synthesis technique [7]. Different investigations have been reported over the years on AgNP production utilizing plant extracts. Some of the earlier investigations revealed a green synthesis of AgNPs with the aid of *Lantana camarader* [8], *Parkia speciossa* hask pod [9], apple extract [10], *Buddleja globosa* hope [11] and *Azadirachta indica* [12]. Some research has shown that the biological/chemical activities of AgNPs are closely linked to the

physicochemical properties of AgNPs. Several researches stated in (Table 1) show that the molar ratio is a key parameter for forming the particle size when employing plant extract for $AgNO_3$ synthesis, rather than for the technique used for the manufacture of nanoparticles. An interesting subject is the exploration of various plant extracts for the AgNPs production [13-15].

By reviewing prior research that revealed the usage of red type spinach (*Amaranthus Tricolor L.*) to provide a secondary metabolite of the chemicals. present research looks at using Green *Spinicia oleracea* leaf extract as a reducing agent in the manufacture of AgNPs. This research focuses on the extraction, optimization, synthesis, and assessment of antibacterial properties of produced AgNPs [16-18].

Materials and Methods

Materials

The analytical grade of all reactants in this investigation is utilized without any additional purification. Silver nitrate ($AgNO_3$) was purchased from (Avonchem limited UK) and Merck-Millipore supplied the distilled water (Germany). *Spinicia oleracea* green leaf extract was collected in Baghdad, Iraq, from a local market. The soaking process was used to create *Spinicia oleracea* leaf extract (GSE). Overnight, 50g dry green spinach leaves were soaked in roughly of water (100ml) solvent. GSE was extracted from the combination by filtering the solution. in an oven the soaking extract was then dried at 50 °C and 1 gram of the powder produced after drying was weighed and analyzed in 50ml of distilled water to dilute the extract with diluted silver nitrate in a molar ratio specified for the purpose of research.

Synthesis of AgNPs

Silver nanoparticles have been synthetized by mixing $AgNO_3$-10^{-2}M with GSE at a constant volume ratio of 20%. The blend was handled for 5 hours at room temperature to guarantee a reduction reaction between Ag^+ and Ag^0 [19]. The decline study was confirmed by UV-Visible spectroscopy. Analyzer of particle size, infrared microscope and Transmission-Electron Microscope (TEM) Fourier transform was used to further investigate the AgNPs. For these tests, the Particle Size Analyzer HORIBA and the JEOL TEM apparatus were used with a dynamic light dispersion system operating at 120kV. In order to ensure that the single phase of Ag is acquired from synthesis, the Perkin–Elmer spectrometer equipment was used and X-Ray Diffractors (XRD) analysis was carried out using the Shimadzu X6000 equipment, which operated as a radiation source with the Ni filtered CuKα.

Antibacterial activity test of AgNPs

Using the well diffusion experiment, the antibacterial activity of produced AgNPs was determined. Synthesized AgNPs with stock concentration (500µg/ml) and dilutions (250, 125µg/ml) was used to detect the antibacterial activity. The bacterial culture in the McFarland turbidity tube was activated for 18 hours in nutritional broth at 37 pounds in a McFarland turbidity tube with a concentration of 1.5*108 cells/ml. At 18hr, pathogenic bacteria (*Escherichia coli*) were active at 37LC. Pathogenic bacteria utilizing cotton swab have been injected on sterilized nutrient agar plates. The wells were cut off by using a sterile pipette of a pasture after 5-10 minutes. At each concentration, agNPs solution (100µL) has been applied to the well and incubated for 24 hours at a temperature of 37 °C. Inhibition areas were measured in mm after the incubation period [20].

Results and Discussion

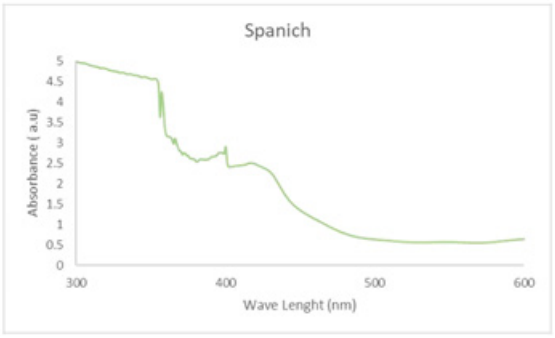

Figure 1: UV-visible AgNP spectrum synthesized.

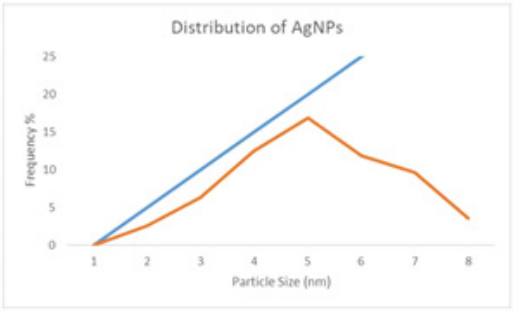

Figure 2: Particle size distribution of AgNPs.

Depicts the UV-visible spectra of produced AgNP at various GSE volumes, (Figure 1). GSE shows specific wavelengths in the range 300-350nm and the strong spectrum 406nm. These spectrums are connected to the presence of RSE anthocyanine and phenolic compounds, which is consistent with previous research [21]. All AgNPs have a maximum wavelength of between 390 and 430nm, which indicates Surface Resonance (SPR). In order to indicate the Surface Plasm Resonance (SPR) absorption range, AgNPs shows a maximum wavelength in the 390-430nm region. The electronic UV-visible light wavelength of the nanosized Ag is related to these SPR absorption bands. Additionally, all samples of AgNPs show the presence of polyphenols or aromatic molecular structures of GSE at peaks at approximately 300-340nm. Given that each AgNP sample demonstrates a single SPR band, the nanoparticles are projected to be spherical, whereas the nanoparticles correspond to the anisotropic molecules, as there are two and more SPR bands

Copyright © Mohammed RA

[22]. It was proven that the greater GSE size percentage delivers the larger maximum wavelength with the broader area after executing multiple trials to acquire the optimal GSE size % and via the researchers' earlier investigations. AgNPs-2 produced the most intense spectrum associated with SPR production. The examination of particle size ensures the average distribution of particle size and particle sizes. (Figure 2) displays distribution curves and (Table 2) tabulates the average particle size figures. The GSE volume percent (16.45nm) with lesser polydispersion (PI) value (PI=0.063) was used to achieve the uniform size of particulate matter. The larger the GSE volume, the larger the average particle size and the PI show the widespread size. This behavior is in accordance with the UV spectrum and can lead to greater particle sizes at higher GSE levels [11,23].

Table 1: Some studies on silver nanoparticles biosynthesis.

Plant extract	Particle size (nm)	Results	References
Buddleja globosa	15-16	The low-cost and effective technique of silver nanoparticle production is provided via biosynthesis and low-concentration extracts.	11
Origanum vulgare L.	11.21	Increased toxicity in many microorganisms, including bacteria and fungi such as: *Shigella sonnei, Micrococcus luteus, Escherichia coli, Aspergillus alternata, Paecilomyces variotii and Phialophora alba. Alternaria alternata*	13
Eriobotrya japonica	21	AgNPs were shown to be efficient against *E. coli* and *Staphylococcus aureus*	14
Crocus sativus L.	21-Nov	AgNPs have exhibited an anti-*E. coli, Pseudomonas aeruginosa, Klebsiella pneumoniae, Shigella flexneri* and *Bacillus subtilis activity*	15
Alpinia katsumadai	44.83–123.2	The activity and antibacterial activity against *E. coli* and *S. aureus* were shown by AgNPs	16
Alpinia katsumadai	12.5	Against *E. coli* and *S. aureus,* AgNPs demonstrated unique free radical scavenging and strong antibacterial action.	18
Azadirachta indica	33	AgNPs were shown to have antibacterial properties against Gram-positive (*S. aureus*) and Gram-negative *(E. coli)* pathogens.	12
Parkia speciossa Hask pod	105-161	The synthesized method: reflux, microwave and sonication affect the size of the part of AgNPs.	11
Convolvulus arvensis	90.8nm	In presence of $NaBH_4$, preparation of AgNPs has the potential to reduce azo dyes in catalysts.	17
Artemisia vulgaris	26	Effective antibacterial action against *E. coli, P. aeruginosa, K. pneumoniae* and Haemophilus influenzae was exhibited in synthesized nanoparticles	18

Table 2: Synthesized AgNP particle size data.

Sample	AgNPs-2
Particle size	16.45
PI	0.063

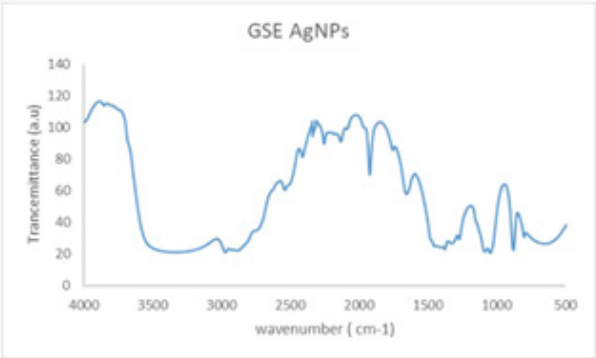

Figure 3: The FTIR spectra of produced AgNPs were compared to those of GSE.

(Figure 3) shows the AgNPs-20% and GSE FTIR spectrums. The presence of (O–H) functional group in GSE samples shows prominent absorbance bands detected at around 3100–3900cm^{-1}. Other high points at 1661 and 1926, 2538 and 2972cm^{-1} was detected, respectively, indicating –C=O, -O--C, and alkane (C–H). C–C and C–N vibrations of the tetrapyrrole ring of chlorophyll, which are connected with a UV–visible vibration, are principally related to the peaks of ν~1049cm^{-1} and ν~1381cm^{-1}. The absorption spectrum found is comparable to the FTIR spinach extract analysis [24]. These findings are comparable to earlier AgNP biosynthetic extract research [8]. (Figure 4) shows the spherical form of nanoparticles between 2-41nm in the image of the spinach extract with AgNP. The findings fit into the distribution of particulate size and UV-visional AgNP spectrum that indicates the nanoparticles' size range. The particles are also evident when the organic material from the plant extract is covered by a thin coating. The organic cap material aids in the stabilization of nanoparticles. The existence of organic material has been also shown by the X-ray spectrum energy dispersion of AgNPs, which displays Ag, C and O existence. As capping AgNPs, the C and O signals derive from organic GSE molecules. There is no N signal that indicates the lack of $AgNO_3$ since the Ag^+ production is completely reduced. The measurement of XRD was conducted in order to ensure the synthesis of the single AgNP material produced. The reflex spectrum of filtered AgNPs is shown in (Figure 5). Four strong peaks are shown in the XRD pattern with 2θ values between 30 and 70. Intense peaks at 2θ point values are in the range of 31.9,

Copyright © Mohammed RA

43.31, 60.4 and 63.4 (111), (200), (220) and (311) according to JCPDS, silver file 04-078 [25].

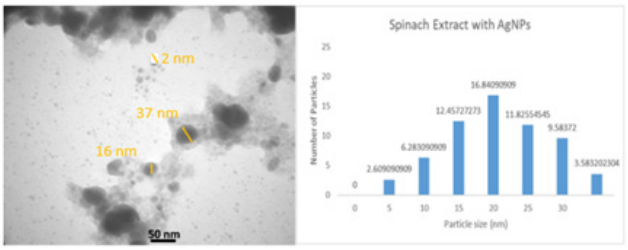

Figure 4: TEM image of AgNPs synthesized.

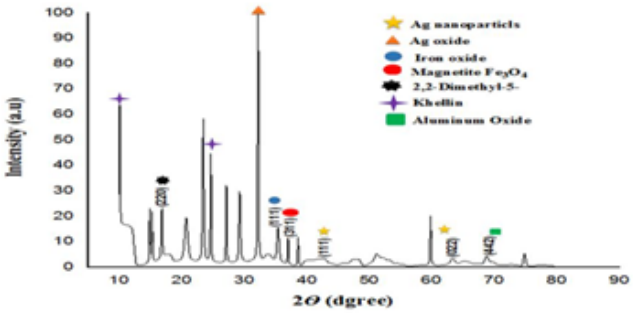

Figure 5: Image of XRD pattern of AgNPs synthesized.

Table 3: Inhibition zone of antibacterial activity test of synthesized GRE AgNPs.

Sample	Measurement 1(mm)	Measurement 2(mm)
GRE AgNPs	32.1	31.7
Amoxicillin	19.6	19.3
Water	1.3	1.3

GRE AgNPs have been studied for their antibacterial effects, and the results were presented in (Table 3), which included a comparison of the inhibition areas in the samples for GRE, as well as with amoxicillin as a positive control and with water: ethanol (1:1) as a solvent GRE, where the obtained area indicates that the maximum Antibacterial activity is what was extracted and prepared from a sample of GRE AgNPs. The antibacterial activity increases with the proportion of GRE, which is likewise consistent with the rising particle size average. The volume ratio of silver nanoparticles concentration has no effect on the inhibition zones because it works in principle on the size of the obtained nanoparticles with the effect of the extract on the sizes of these particles, which means that the nanoparticles have no effect on the antibacterial activity at different GRE percentages. These results show that particle size has an influence on antibacterial activity, with smaller particles being more effective [26]. The smaller size aids in more efficient penetration of the bacterium cell membrane for subsequent degradation of sulfur- and phosphorus-containing complexes such as DNA and causing cell death [22].

For synthesizing nanoparticles many plant components or complete plants are utilized [27]. Differences in the size or form of the produced nanoparticles in inhibition diameters might be attributed to differing effects on bacterial growth and causing inhibition [25]. Such formulations can be utilized for numerous biotechnological applications and medicinal purposes to destroy harmful microorganisms. The small size and high surface to volume ratio was related to their bactericidal effect of metal nanoparticles, which let them interact with microbial membranes and other contents of the bacterial cell [28]. Antimicrobial feature of the AgNPs are the positive charges and the ionized silver form. These ions develop complications with DNA, notably nucleosides, and other bacterial cell components [29]. Studies have demonstrated that electrostatic interaction exists between positively charged Nanoparticles (NPs) and negatively charged bacterium cells as a bactericidal agent. These NPs build up within bacterial membranes, infiltrate bacterial cells, cause harm, and eventually kill them [30]. Some studies have demonstrated that the silver atoms connect to (-SH) the group of bacterial enzymes, causing stable S-Ag bonds that result in enzyme deactivation, while others have suggested that silver ions entering cells interrupt the base pairs of pyrimidines and purines, causing hydrogen bond interruption between the parallel DNA strands and eventually causing denaturization. The interaction with bacterial cell macromolecules includes the process of electron release and free radical production [31]. Inhibit protein and cell wall production inducing NPs is caused by buildup of precursor envelope proteins, external membrane disruption, and finishes by energy leakage [32]. As shown in (Figure 6) depicts the efficacy of the GRE plant extract with AgNPs on the bacteria used, as well as the antibacterial activity of the GRE AgNPs depending on the size of the silver nanoparticles, which were finally formed with the extract to give an efficacy of bacterial inhibition due to the small size of these nanoparticles and their penetration into the innovative cell membrane, with an effective diameter of up to 32mm.

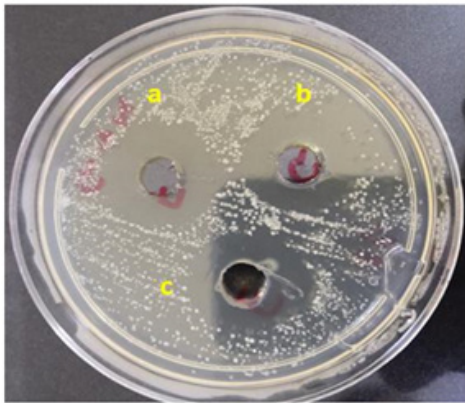

Figure 6: The antibacterial activity of synthesized AgNPs by GRE plant extract against *E. coli*. Inhibition zones according to concentration of synthesized AgNPs; a: 35mm at 500µg/ml, b: 32mm at 250µg/ml, c: 30mm at 125µg/ml.

Copyright © Mohammed RA

Conclusion

The use of Green Spinach leaf extract as a bio reduction was effectively produced in silver nanoparticles (AgNPs). The analysis of UV-visible Spectrophotometry, FTIR and XRD indicate that Ag-NPs are produced from the full Ag+ reduction of $AgNO_3$ nano-size precursor. The volume percentage of GSE is shown to impact the average and distribution of different particle sizes. The effective capping and stabilizing characteristics of the AgNPs were shown in the FTIR, EDX and SEM analyzes. In addition, the synthesized AgNPs showed antibacterial activity against *E. coli*, with the tendency to enhance antibacterial activity as a consequence of smaller particle size.

Funding

This work was supported by Science of Physics Dept. & Science of biology Dept. College of Science, University of Baghdad and Ministry of Higher Education and Scientific Research (IQ).

References

1. George MS, Negandhi P, Farooqui HH, Sharma A, Sanjay Zodpey (2016) How do parents and pediatricians arrive at the decision to immunize their children in the private sector? Insights from a qualitative study on rotavirus vaccination across select Indian cities. Hum Vaccin Immunother 12(12): 3139-3145.
2. Walker CLF, Black R (2011) Rotavirus vaccine and diarrhea mortality: Quantifying regional variation in effect size. BMC Public Health 11(3): 1-7.
3. Lamberti LM, Ashraf S, Walker CLF, Black RE (2016) A systematic review of the effect of rotavirus vaccination on diarrhea outcomes among children younger than 5 years. Pediatr Infect Dis J 35(9): 992-998.
4. Dubé E, Bettinger JA, Halperin B, Bradet R, Lavoie F, et al. (2012) Determinants of parents' decision to vaccinate their children against rotavirus: Results of a longitudinal study. Health Educ Res 27(6): 1069-1080.
5. Tate JE, Burton AH, Boschi-Pinto C, Steele AD, Duque J, et al. (2012) 2008 estimate of worldwide rotavirus-associated mortality in children younger than 5 years before the introduction of universal rotavirus vaccination programmes: A systematic review and meta-analysis. Lancet Infect Dis 12(2): 136-141.
6. Bar-Zeev N, Kapanda L, Jacqueline ET, Khuzwayo CJ, Iturriza-Gomara M, et al. (2015) Effectiveness of a monovalent rotavirus vaccine in infants in Malawi after programmatic roll-out: An observational and case-control study. Lancet Infect Dis 15(4): 422-428.
7. Abeid KA, Jani B, Cortese MM, Kamugisha C, Mwenda JM, et al. (2017) Monovalent rotavirus vaccine effectiveness and impact on rotavirus hospitalizations in Zanzibar, Tanzania: Data From the first 3 years after introduction. J Infect Dis 215(2): 183-191.
8. Ruiz-Palacios GM, Pérez-Schael I, Velázquez FR, Abate H, Breuer T, et al. (2006) Safety and efficacy of an attenuated vaccine against severe rotavirus gastroenteritis. N Engl J Med 354(1): 11-22.
9. Linhares AC, Velázquez FR, Pérez-Schael I, Sáez-Llorens X, Abate H, et al. (2008) Human rotavirus vaccine study group efficacy and safety of an oral live attenuated human rotavirus vaccine against rotavirus gastroenteritis during the first 2 years of life in Latin American infants: A randomised, double-blind, placebo-controlled phase III study. Lancet 371(9619): 1181-1189.
10. Deen J, Lopez AL, Kanungo S, Wang X, Anh DD, et al. (2018) Improving rotavirus vaccine coverage: Can newer-generation and locally produced vaccines help? Hum Vaccin Immunother 14(2): 495-499.
11. Lopez AL, Daag JV, Esparagoza J, Bonifacio J, Fox K, et al. (2018) Effectiveness of monovalent rotavirus vaccine in the Philippines. Scientific Reports 8(1): 1-8.

For possible submissions Click below:

Submit Article